Carotene as a Molecular Wire: Conducting Atomic Force Microscopy

G. Leatherman,[†] E. N. Durantini,[‡] D. Gust,[‡] T. A. Moore,[‡] A. L. Moore,[‡] S. Stone,[‡] Z. Zhou,[‡] P. Rez,[†] Y. Z. Liu,[†] and S. M. Lindsay*[,†]

Department of Physics and Astronomy and Department of Chemistry and Biochemistry, Arizona State University, Tempe, Arizona 85287

Received: July 22, 1998; In Final Form: September 16, 1998

A conducting atomic force microscope was used to measure the electrical properties of carotenoid molecules attached to a gold electrode. The thiolated carotene molecules were embedded in insulating *n*-alkanethiol self-assembled monolayers. At a contact force of a few nanoNewtons, a carotenoid molecule behaves ohmically with a resistance of approximately 4.2 ± 0.7 GΩ, over a million times more conductive than an alkane chain of similar length. Modes of electron transport are discussed.

Introduction

Current proposals for molecular wires include organic molecules with large, delocalized π-electron systems.[1] The prototypical natural molecular conductor of this type is the carotenoid polyene. Much of the color in plants, animals, and microorganisms is due to the absorption of light by carotenoids, whose optical properties arise from electronic states that are delocalized over a chain of some twenty carbon atoms connected by alternating single and double bonds.[2,3] Carotenoids are readily oxidized electrochemically,[4,5] implying that they can be charged at a metal surface, and in their ionic states, charge is delocalized over the length of the conjugated chain. Photoinduced electron transfer through carotenoids is facile.[6,7] These facts suggest that single carotenoids fixed between metallic contacts could function as wires. In this work, conducting atomic force microscopy has been used to contact individual carotenoids embedded in an insulating alkanethiol monolayer on a gold surface with a controlled force so as to measure the resistance of the molecule.

The scanning tunneling microscope has been used to measure the electrical properties of small molecules[8,9] and nanostructures such as carbon nanotubes.[10] Oxidation currents have been detected from single molecules in solution.[11] Atomic "wires" have been fabricated by stacking Xe atoms on top of one another with an STM tip.[12] The resistance of such a two atom "wire" was 10^7 Ω. A combined STM-microwave dielectric microscope was used to detect conduction in 4,4′-di(phenylene-ethynylene)-benzenethiolate.[13] Molecules have been strung across micro-fabricated junctions[14] and coated onto microcracks ("break-junctions") in electrodes.[15] These methods present some difficulties. In STM-based experiments, the contact force is not controlled. The electronic properties of a molecule are sensitive to the effects of deformation[16−18] so it is important to sense force and current simultaneously. This has been accomplished in this work by the use of a conducting atomic force microscope (AFM) to image and contact individual molecules embedded in an otherwise insulating film. Contamination by water adlayers and molecular oxygen can lead to spurious conductivity signals[19] so our measurements were carried out under an inert atmosphere with the sample and probe covered by an insulating liquid.

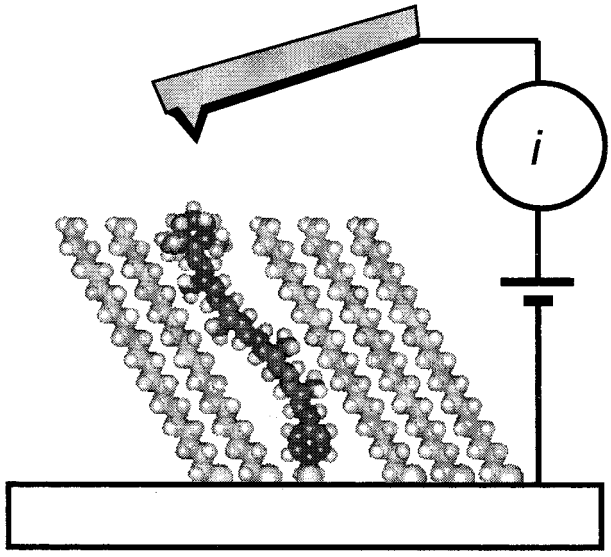

Figure 1. Schematic illustration of the experiment. Structural models are for the carotenoid embedded in 1-docosanethiol attached to a gold surface. Current flow is measured between a biased Pt-coated AFM cantilever and a gold substrate. The tip is grounded and a bias applied to the substrate. The sample is submerged in an insulating solvent in a clean Teflon container.

Experimental Section

Synthesis. The carotenoid, (7′-apo-7′-(4-iodomethylphenyl)-β-carotene), was synthesized as described below and mixed with either 1-dodecanethiol (12 carbon atoms, Aldrich Chemical Co.) or 22-carbon diluent, 1-docosanethiol (see below), in toluene solutions. The alkanethiols formed ordered monolayers in which carotenoids were embedded as illustrated in Figure 1, which shows the overall layout. The structure of the carotenoid is illustrated below:

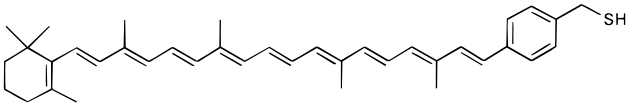

The thiols were synthesized from the corresponding halide, 7′-apo-7′-(4-iodomethylphenyl)-β-carotene[20] or 1-bromo-

* Corresponding author. E-mail: Stuart.Lindsay@ASU.EDU.
[†] Department of Physics and Astronomy.
[‡] Department of Chemistry and Biochemistry.

10.1021/jp9831278 CCC: $18.00
Published on Web 00/00/0000 PAGE EST: 5

docosane, by nucleophilic displacement of the halide with an excess of thiourea in THF. The thiols were obtained by base hydrolysis of the thiouronium salt.

All materials were characterized by ^{1}H and ^{13}C NMR (COSY, HMBC, and HMQC). The spectra were recorded on a Varian Unity spectrometer at 500 MHz. The samples were dissolved in deuteriochloroform with tetramethylsilane as an internal standard. Mass spectra were obtained with a matrix-assisted time-of-flight spectrometer (Vestec Laser Tec Research Instrument using a sulfur matrix). Measured mass/charge ratios (*m*/*z*) are listed for each compound. 1-Bromodocosane from Aldrich were used as received. Tetrahydrofuran (THF) was distilled from lithium aluminum hydride under an argon atmosphere and used at once.

7′-Apo-7′-(4-mercaptomethylphenyl)-*β*-carotene (1). A portion of 7′-apo-7′-(4-iodomethylphenyl)-*β*-carotene (40 mg, 0.063 mmol) was added to an excess of thiourea (200 mg) in THF (20 mL). The reaction mixture was stirred under nitrogen at room temperature for 20 min. TLC (silica gel, hexane/3% ethyl acetate) indicated that all of the iodocarotene was consumed and the polar thiouronium salt was formed. The reaction mixture was filtered. Powdered KOH (250 mg) was added to the filtrate and the mixture was vigorously stirred under nitrogen at room temperature for 45 min. The crude mixture was diluted with 50 mL of water and extracted with CH_2Cl_2 (3 × mL). The organic phase was dried with $MgSO_4$, filtered and the solvent evaporated under reduced pressure. Flash chromatography on silica gel (hexane/20% CH_2Cl_2) afforded 28 mg (83%) of pure carotenethiol (**1**). MS *m*/*z*: 536 M^+ (536 calculated for $C_{38}H_{48}S$). ^{1}H NMR (500 MHz, $CDCl_3$) δ [ppm] 1.02 (s, 6H, 16-CH_3, 17-CH_3), 1.47 (m, 2H, 2-CH_2−), 1.61 (m, 2H, 3-CH_2−), 1.71 (s, 3H, 18-CH_3), 1.97 (s, 9H, 19-CH_3, 20-CH_3, 20′-CH_3), 2.01 (m, 2H, 4-CH_2−), 2.03 (s, 3H, 19′-CH_3), 3.62 (s, 2H, Ar-*C*H_2−SH), 6.14 (d, 1H, J = 15.5 Hz, 8-CH−), 6.15 (d, J = 8.5 Hz, 1H, 10-CH−), 6.16 (d, 1H, J = 15.5 Hz, 7-CH−), 6.25 (d, 1H, J = 10.5 Hz, 14′-CH−), 6.27 (d, 1H, J = 8.0 Hz, 14-CH−), 6.35 (d, 1H, J = 11.0 Hz, 10′-CH−), 6.37 (d, 1H, J = 15.0 Hz, 12-CH−), 6.41 (d, 1H, J = 15.0 Hz, 12′-CH−), 6.55 (d, 1H, J = 16.0 Hz, 7′-CH−), 6.62−6.66 (m, 4H, 15′-CH−, 15-CH−, 11-CH−, 11′-CH−), 6.88 (d, 1H, J = 16.0 Hz, 8′-CH−), 7.17 (d, 2H, J = 7.5 Hz, ArH), 7.37 (d, 2H, J = 7.5 Hz, ArH). ^{13}C NMR (125.75 MHz, $CDCl_3$) δ [ppm] 12.70 (19-C, 20-C, 19′-C, 20′−C), 19.10 (3-C), 21.61 (18-C), 32.93 (4-C), 34.30 (1-C), 39.45 (2-C, 16-C, 17-C), 43.17 (21-C), 124.47 (11′-C), 125.25 (11-C), 126.32 (C-Ar), 126.68 (7-C), 126.87 (7′-C), 129.34 (5-C), 129.71 (C-Ar), 130.13 (15-C), 130.40 (15′-C), 130.67 (13′-C), 130.73 (10-C), 132.34 (14′-C), 132.50 (13-C), 133.20 (14-C), 133.23 (10′-C); 133.77 (8′-C), 135.40 (9′-C), 136.00 (C-Ar), 137.00 (C-Ar), 137.19 (12-C), 137.68 (8-C), 137.87 (6-C), 138.34 (9-C), 138.47 (12′-C).

1-Docosanethiol. It was synthesized as described for **1** using 1-bromodocosane (500 mg, 1.28 mmol) and thiourea (2 g) in THF (100 mL). The reaction mixture was stirred under nitrogen at 80 °C for 18 h. TLC (silica gel, hexane) indicated that all of the alkyl bromide was consumed. The suspension was filtered, and the THF solution was stirred under nitrogen with powdered KOH (2 g) at 80 °C for 30 min. The crude mixture was diluted with 150 mL of water and extracted with CH_2Cl_2 (3 × 100 mL). Flash chromatography on silica gel (hexane) yielded 354 mg (81%) of 1-docosanethiol. MS *m*/*z*: 342 M^+ (342 calculated for $C_{22}H_{46}S$). ^{1}H NMR (500 MHz, $CDCl_3$) δ [ppm] 0.86 (t, 3H, J = 6.6 Hz, −CH_3), 1.18−1.36 (m, 38H, −CH_2-), 1.32 (t, 1H, J = 7.2 Hz −SH), 1.60 (q, 2H, J = 7.2 Hz *C*H_2−CH_2−SH), 2.52 (q, 2H, J = 7.2, −CH_2−SH).

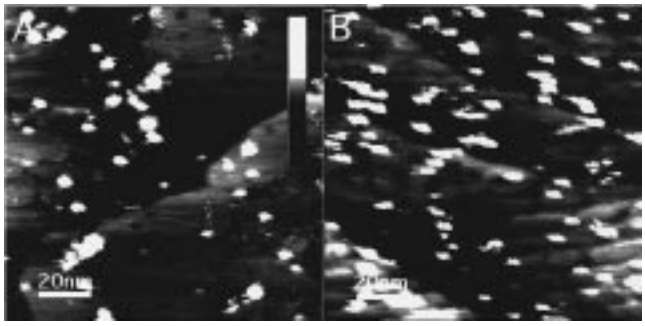

Figure 2. (A) STM image of film made from a toluene solution containing 1 mM 1-dodecanethiol + 0.003 mM carotenethiol: (B) as in A with 0.015 mM carotenethiol. Images taken in constant current mode at 5 pA and +800 mV. Height scale for both images (shown in A) is 0 to 3 nm.

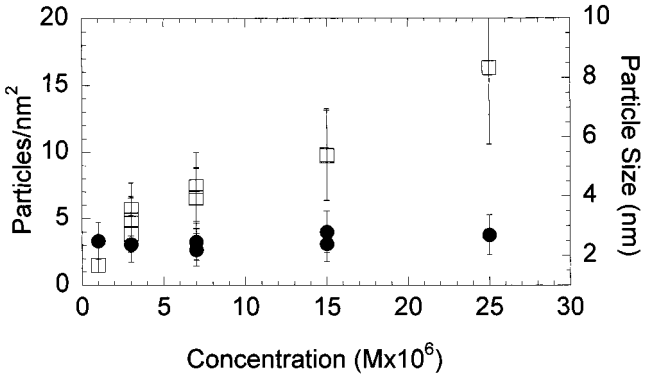

Figure 3. Coverage of carotenethiol (left scale, open squares) and particle size (right scale, filled circles) as a function of carotenoid solution concentration.

Sample Preparation and Imaging. Solutions of the carotenoid and either 1-dodecanethiol or 1-docosanethiol in freshly distilled toluene were placed on freshly flame-annealed[21] films of Au(111) on mica[22] and left to adsorb for ca. 1 h. Samples were then rinsed with freshly distilled toluene and imaged under the same solvent in a dry-nitrogen environment.

The conducting AFM (PicoSPM, Molecular Imaging, Tempe, AZ) has a force-sensing cantilever coated with platinum and connected to a low-noise current amplifier. The amplifier has a sensitivity of 1V/nA and a noise level of 0.01 pA/$\sqrt{\text{Hz}}$. Cantilevers, of nominal force constant 0.05N/m, were supplied sputter-coated with platinum by Molecular Imaging. The AFM is operated in the conventional constant force contact mode to produce a topographic image of the sample, while the current signal is fed to a second input channel of the controller, simultaneously producing a conductivity map.

Results

STM images of films made from solutions with increasing concentrations of carotenoid in 1-dodecanethiol showed an increasing density of bright spots over the otherwise normal background images owing to the ordered alkanethiol monolayers. Typical images at two concentrations are shown in Figures 2A and B. Note that the apparent size of the spots does not appear to change with dose while the coverage increases in these images. The spot size is highly variable, being dominated by the geometry of the tips. Data from many such runs (summarized in Figure 3) show that the size is, on average, about 2 nm, independent of carotenoid concentration. Figure 3 also shows how the number of bright spots increases smoothly with

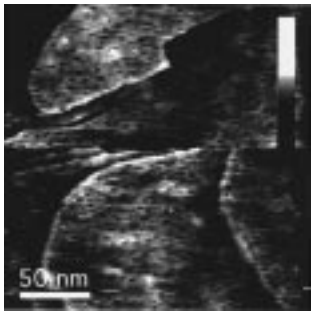

Figure 4. AFM image of a film on Au(111) prepared from a toluene solution containing 1 mM 1-docosanethiol. Height scale is 0 to 50 nm.

carotenoid concentration up to 2.5×10^{-5} M in the application solution. These data indicate that over this range of concentration, the carotenoid probably resides in the film as isolated molecules and not as aggregates. We cannot rule out the possibility of a small aggregate (e.g., two molecules) of constant size, but this seems unlikely.

Attempts to obtain reproducible current−voltage characteristics from carotenoids in dodecanethiol films were not successful, presumably because the much-longer carotenoid molecules protrude from the surrounding film and were moved or damaged during the scans. Reproducibility was greatly improved when carotenoid molecules were embedded in monolayers of 1-docosanethiol, molecules of similar length to that of the carotenes (see Figure 1).

These much longer alkanes form densely packed monolayers which display the pits observed in monolayers made from shorter alkanethiols[23] and a typical AFM image of pure 1-docosanethiol is shown in Figure 4. The film is quite ordered at the molecular level, even at high levels of carotenoid doping as shown by the molecular-resolution scan in Figure 5A. The average alkanethiol nearest-neighbor distance is close to 0.5 nm, as expected, but the lattice is distorted from the near-hexagonal packing found in films made from shorter alkanethiols[24] possibly because these longer molecules are not in an equilibrium packing geometry.

The pure 1-docosanethiol films were insulating up to the highest voltages (±2V) and forces (6nN) applied and could not be imaged by STM. In contrast, films doped with carotenoid showed large current peaks in the conducting AFM images (Figures 5B and C). The density of these peaks was on the same order, at the concentrations used, as those found for the carotenoids in 1-dodecanethiol (Figure 2). Two successive current images taken at 0.25 and 0.40V are shown in Figure 5 for the film prepared from a 0.025mM carotenoid solution. Individual "bright spots" in this scan can be imaged repeatedly, and show a marked increase in intensity when the bias is increased from 0.25 to 0.40V.

Quantitative analysis of the "current spots" associated with the carotenoids is complicated by two factors. First, the current through a molecule is known to depend on the force used to contact the molecule.[17,18] Application of a bias to the tip will generate an electrostatic force between the tip and sample[25] resulting in a spurious bias dependence of the current. Second, the shape and overall intensity of the spot clearly depends on the geometry of the tip.

The dependence of current on force is illustrated in Figure 6 which shows a measure (I_m, see below) of the peak spot intensity plotted against the set-point force. The presence of an electrostatic force between the cantilever and sample is evident on examination of the force−distance plot obtained on approaching the surface. A typical example is shown in Figure 7A. Curves such as this were well fitted by an inverse square law

$$F = \frac{A}{(Z - Z_0)^2} \tag{1}$$

where Z is the distance from the nominal contact point (where the tip snaps into contact). Curves could be fitted with $Z_0 = -300$ nm, so we fixed this parameter and extracted A as a function of tip bias. These values for A as a function of bias are shown in Figure 7B. They fit a parabola, as expected for a Coulomb interaction.[25] The center of the parabola is offset from zero volts indicating that the film is intrinsically positively charged. We observed similar behavior at many points on the film, regardless of the carotenoid concentration (which is small in any case) so we conclude that this charge is an intrinsic property of the alkanethiol monolayer. It is more difficult to understand the large negative value for Z_0 as this would locate the charge well within the metal if a point-charge model were applied. This difficulty might be remedied by a more accurate model of the charge distribution on the tip, as the weighted center of the tip charge undoubtedly lies some distance above its apex. Thus, when the tip contacts the surface, the center of the charge distribution is some distance above the surface.

The electrostatically generated force was compensated for by adjusting the set-point of the microscope each time the voltage was changed. Specifically, the extra (attractive) deflection owing to the voltage change was noted and the tip pulled back by an equivalent amount so as to compensate for the added electrostatic force. The effect is quite small for the tips used in these experiments, but becomes more important when sharper tips are used.

Analysis of these images must take account of the current distribution around each spot in the image. We expect that the current will vary from a maximum at the center of the tip because of the variation in the molecular distortion as the molecule passes under different parts of the tip that are embedded in the film.[17] This is illustrated in the inset in Figure 8. For a tip with axial symmetry, the number of pixels, ΔN, at a given radius, r, from its axis varies as $\Delta N = Br$ where B is a constant. Given a power-law dependence of current on force (proportional to h, the indentation of the film, inset in Figure 8), and a monotonic decrease of local force with increasing r (decreasing h) we obtain $I \approx E - FN^p$ where E, F, and p are constants. In practice, a simple power-law fits the data quite well. This is illustrated by two representative data sets in Figure 8 where we have plotted the natural logarithm of the number of pixels in a given current interval against the natural logarithm of the current (in picoamps) for a given spot at two values of substrate bias. The intercept at $\log_e(\Delta N) = 0$ corresponds to the maximum current under the tip I_m. While I_m could have been selected from the data, the fitting procedure has the advantage that all of the pixels in a spot are used in deducing its value, and more reproducible data are obtained. The same analysis cannot be applied to whole images because the number of molecules contacted tends to decrease with repeated scanning, presumably because of tip-induced damage. Accordingly, a histogram of the number of pixels corresponding to a given current interval was constructed for each current spot in an image, and I_m was deduced from a regression analysis of a plot of the logarithm of the current vs the logarithm of the number of pixels. Many (ca. 50) spots were analyzed at each value of bias. We changed the bias in a randomized sequence, stepping from positive to negative values, and checking that values were consistent with data recorded earlier in order to ensure that the

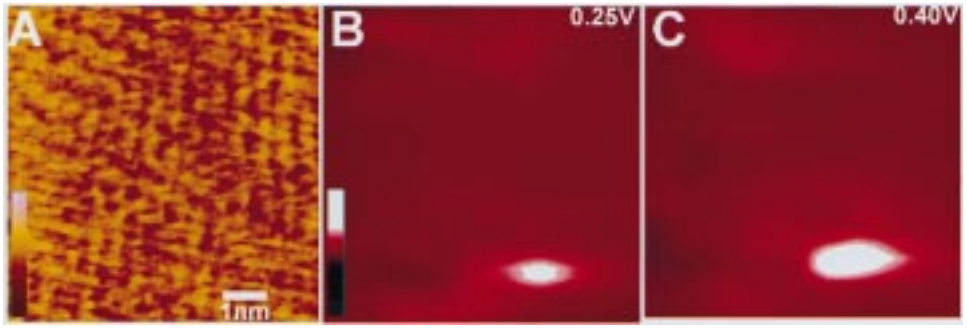

Figure 5. (A) Molecular resolution AFM image of a film prepared from a toluene solution containing 1 mM 1-docosanethiol + 0.025mM carotenoid. (B) Current image of the same film at substrate bias = +0.25 V. (C) As in (B) with bias = +0.40 V. Height color scale shown for A is 1 nm. Scale bar for B and C is 0 to 16 pA. Horizontal scale scale for all 3 images is given in A. Contact force for all three images was set to 3 nN.

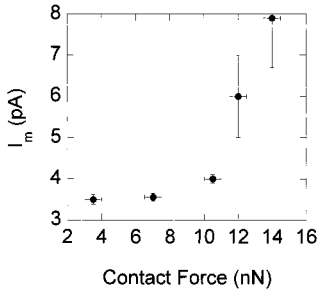

Figure 6. Maximum current (I_m) as a function of contact force for substrate bias = +0.3 V for carotenoid in 1-docosanethiol (error bars are ± standard error).

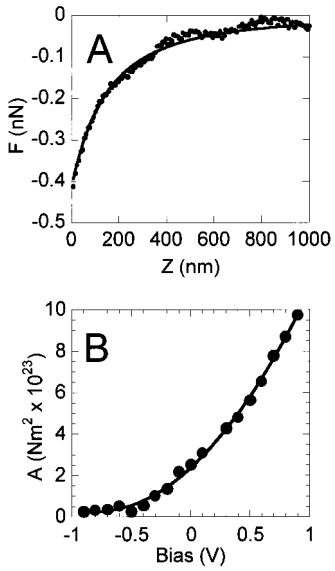

Figure 7. Electrostatic interaction between tip and sample. (A) Shows long-range attractive force for +300 mV sample bias. Solid line is fit to inverse square law. (B) Shows interaction strength parameter *A* as extracted from fits to force distance curves. Solid line is fit to a parabola with zero charge at −0.9 V.

data were reproducible. We checked that the shape of the I−V curve we deduced in this way was independent of the power-law model by analyzing the data for each molecule in terms of a current density over an arbitrarily chosen 2 nm diameter circle, obtaining a similar form for the current−voltage plot.

Results for three different sample preparations using three different tips are shown in Figure 9.

Discussion

The carotenethiol molecules do indeed act as molecular wires, behaving like a 4.2 ± 0.7 GΩ resistor (the heavy straight line

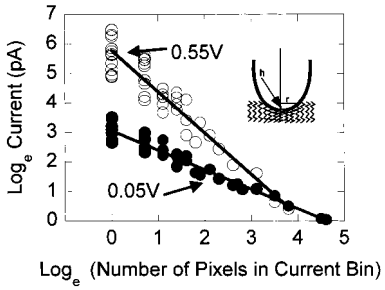

Figure 8. Natural log of current vs the natural log of the number of pixels in a given current interval. Data are for one spot at two values of substrate bias (as marked). The current at $\log_e(\Delta N) = 0$ is I_m, the maximum current under the apex of the tip. The insert shows the model of film deformation on which this extrapolation is based. h is the maximum indentation of the film at the apex of the tip.

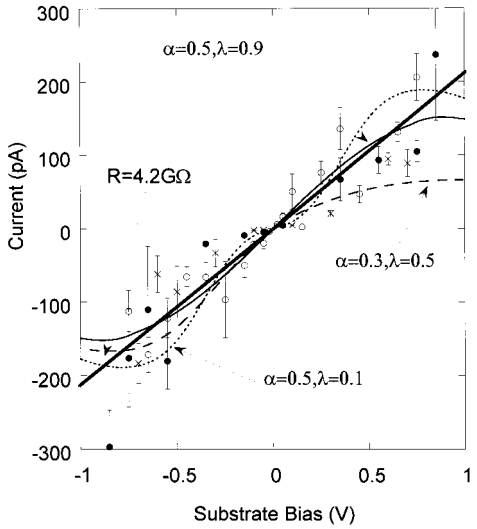

Figure 9. Data for I_m as a function of substrate bias for three different sample preparations (open and closed circles and crosses). Contact forces are 3 nN (O and ×) and 8.5 nN (●). The error bars are ±1 standard error calculated from the measured distributions. The thick solid line is a best fit to a simple ohmic model and the thin lines are fits to a two-step electron-transfer model for values of α and λ as shown and a potential difference between the mean Fermi energy and oxidation level of 0.28V.

in Figure 9) over a range of ±1V. We could measure no current through the 1-docosanethiol films, but, given the measured resistance of decanethiol monolayers (3×10^{10} Ω[24]) and a current-decay coefficient per CH_2, β, of 1.06[26] we estimate their resistance to be about 10^{16}Ω. Thus, the carotenethiol molecules are over a million times more conductive than an alkane chain of similar length, but still 10^4 times less conductive than an ideal quantum wire.[27]

Carotenethiol is easily oxidized electrochemically (+0.53V vs SCE) and we expect that oxidation (hole transport) plays a role in the enhanced conductivity of carotene. We have recently reviewed the tunneling behavior of electroactive molecules.[8] Han et al. [8] give expressions for the tunnel current as a function of bias for a one-step model (the electron tunnels through the unrelaxed molecular levels without occupying them) and a two-step model (the electron occupies the molecular orbitals long enough for relaxation to occur). The key parameters are E_0, the formal potential relative to the mean Fermi energy of the tip and substrate, λ, the electronic reorganization energy, and α, the fraction of the tip−substrate bias that appears across the molecule-to-substrate gap ($1 - \alpha$ being the fraction dropped across the tip-to-molecule gap). Dropping the approximation of high bias used in our earlier work,[8] the expression for net current flow for the two-step model is

$$I(V) \propto \frac{R_{sm}R_{mt} - R_{tm}R_{ms}}{R_{sm} + R_{tm} + R_{ms} + R_{mt}} \qquad (2)$$

where R is a tunneling rate and the subscripts m, s, and t refer to the molecule, substrate and tip. The R values are calculated from the integrals given by Han et al.[8] The first step in estimating E_0 is to obtain the Fermi energy of the combined tip−substrate system in volts vs SCE. The geometric mean of the values for the work function of Au(111) (5.31V) and polycrystalline Pt (5.65V) yields the work function of the combined system. The work function of the SCE is 4.67 V, giving the Fermi energy of the tip−substrate system as +0.81 V SCE. The formal potential for the first oxidation of the carotenethiol was measured by cyclic voltammetry to be +0.53V vs SCE so that $E_0 = +0.28$V. Calculated curves for some values of α and λ (as marked) are shown in Figure 9. The symmetric behavior of the curve ($I(V) \approx I(-V)$) restricts α to a value near 0.5 (poor fits are obtained below 0.4 or above 0.6). This is surprising, given the difference between the molecule−substrate and molecule−tip junctions, but a similar result was obtained by Datta et al.[9] for tunneling through xylyldithiol. It contrasts with a value near unity for tunneling through porphyrin molecules attached to gold.[8] Our data do not resolve the fine structure needed to discriminate between extreme values for λ. For the same reason, we cannot discriminate between the one- and two-step model.

Finally we note that there is considerable variation in the current measured from molecule to molecule and from the same molecule from scan to scan (reflected in the relatively large standard error bars in Figure 9). This suggests that a significant fraction of the observed resistance originates from the tip-to-molecule contact, an observation at odds with the conclusion that $\alpha = 0.5$. Further systematic studies of the dependence of the resistance on molecular structure are needed to elucidate this point.

Conclusions

Carotenoids are excellent conductors of electrons when compared with saturated hydrocarbons, facilitating measurements of the electrical properties of individual molecules in an insulating matrix. Reproducible current−voltage data are obtained over a range of ±1V when the samples are held in an environment that is free of moisture and molecular oxygen. To a first approximation, the molecules act as ohmic resistors, implying that half of the applied potential appears at the molecular orbital. This behavior has been observed in another molecular system, and it may therefore be characteristic of some (but not all) methods of contacting a molecule. The use of a conducting AFM combined with the insertion of the molecule into an insulating matrix makes determination of the electrical properties of linear conducting molecules straightforward. We anticipate that this technique will lead to a deeper understanding of the mechanisms of molecular conduction as different molecular systems are studied in the future.

Acknowledgment. This work was supported by the NSF (Grants DBI-9513233, CHE-9709272, and INT-9600282) and Molecular Imaging Corporation. We acknowledge useful discussions with Nongjain Tao.

References and Notes

(1) Joachim, C., Roth, S., Eds. *Atomic and Molecular Wires*; Kluwer: Dordrecht, 1997; Vol. 341.

(2) Platt, J. R. Electronic Structure and Excitation of Polyenes and Porphyrins. In *Radiation Biology*; Hollaender, A., Ed.; McGraw-Hill: New York, 1956; pp 71−123.

(3) Kohler, B. E. Electronic Properties of Linear Polyenes. In *Conjugated Polymers*; Brédas, J. L., Silbey, R., Eds.; Kluwer: Dordrecht, 1991; pp 405−434.

(4) Jeevarajan, A. S.; Khaled, M.; Kispert, L. D. *J. Phys. Chem.* **1994**, *98*, 7777−7781.

(5) Sereno, L.; Silber, J. J.; Otero, L.; Bohorquez, M. D. V.; Moore, A. L.; Moore, T. A.; Gust, D. *J. Phys. Chem.* **1996**, *100*, 814−821.

(6) Benniston, A. C.; Goulle, V.; Harriman, A.; Lehn, J. M.; Marczince, B. *J. Phys. Chem.* **1994**, *98*, 8, 7798−7804.

(7) Wasielewski, M. R.; Johnson, D. G.; Svec, W. A.; Kersey, K. M.; Cragg, D. E.; Minsek, D. E. Long-distance photoinduced electron transfer through polyene molecular wires. In *Photochemical Energy Conversion*; Norris, J., Meisel, D., Eds.; Elsevier: New York, 1989; pp 135−147.

(8) Han, W.; Durantini, E. N.; Moore, T. A.; Moore, A. L.; Gust, D.; Rez, P.; Leatherman, G.; Seely, G. R.; Tao, N.; Lindsay, S. M. *J. Phys. Chem.* **1997**, *101*, 10719−10725.

(9) Datta, S.; Tian, W.; Hong, S.; Reifenberger, R.; Henderson, J. I.; Kubiak, C. P. *Phys. Rev. Lett.* **1997**, *79*, 2530−2533.

(10) Collins, P. G.; Zettl, A.; Bando, H.; Thess, A.; Smalley, R. E. *Science* **1997**, *278*, 100−102.

(11) Fan, F. R. F.; Bard, A. J. *Science* **1995**, *267*, 871−874.

(12) Yazolani, A. I.; Eigler, D. M.; Lang, N. D. *Science* **1996**, *272*, 1921−1924.

(13) Bumm, L. A.; Arnold, J. J.; Cygan, M. T.; Dunbar, T. D.; Burgin, T. P.; Jones, L.; Allara, D. L.; Tour, J. M.; Weiss, P. S. *Science* **1996**, *271*, 1705−1707.

(14) Bockrath, M.; Cobden, D. H.; McEuen, P. L.; Chopra, N.; Zettl, A.; Thess, A.; Smalley, R. E. *Science* **1997**, *275*, 1922−1925.

(15) Reed, M. A.; Zhou, C.; Muller, C. J.; Burgin, T. P.; Tour, J. M. *Science* **1997**, *278*, 252−254.

(16) Lindsay, S. M.; Sankey, O. F.; Li, Y.; Herbst, C. *J. Phys. Chem.* **1990**, *94*, 4655−4660.

(17) Durig, U.; Zuger, O.; Michel, B.; Haussling, L.; Ringsdorf, H. *Phys. Rev.* **1993**, *B48*, 1711−1717.

(18) Joachim, C.; Gimzewski, J. K.; Schlittler, R. R.; Chavy, C. *Phys. Rev. Lett.* **1995**, *74*, 2102−2105.

(19) Anselmetti, D.; Baratoff, A.; Guntherodt, H. J.; Gerber, C.; Michel, B.; Rohrer, H. *J. Vac. Sci. Technol.* **1994**, *B12*, 1677−1680.

(20) Gust, D.; Moore, T. A.; Moore, A. L.; Liddell, P. A. *Methods Enzymol.* **1992**, *213*, 87−100.

(21) Wandlowski, T.; Lampner, D.; Lindsay, S. M. *J. Electroanal. Chem.* **1996**, *404*, 215−226.

(22) DeRose, J. A.; Lampner, D. B.; Lindsay, S. M. *J. Vac. Sci. Technol.* **1993**, *A11*, 776−780.

(23) McDermott, C. A.; McDermott, M. T.; Green, J. B.; Porter, M. D. *J. Phys. Chem.* **1995**, *99*, 9, 13257−13267.

(24) Poirier, G. E.; Tarlov, M. J. *Langmuir* **1994**, *10*, 0, 2853−2856.

(25) Martin, Y.; Abraham, D. W.; Wickramasinghe, H. K. *Appl. Phys. Lett.* **1988**, *52*, 1103−1105.

(26) Carter, M. T.; Rowe, G. K.; Richardson, J. N.; Tender, L. M.; Terrill, R. H.; Murray, R. W. *J. Am. Chem. Soc.* **1995**, *117*, 7, 2896−2899.

(27) Landauer, R. *Philos. Mag.* **1970**, *21*, 863−867.